JOURNAL OF GEOPHYSICAL RESEARCH, VOL. 112, D10S01, doi:10.1029/2006JD007727, 2007

Intercomparison of multiaxis and long-path differential optical absorption spectroscopy measurements in the marine boundary layer

Olga Pikelnaya,[1] Stephen C. Hurlock,[1] Sebastian Trick,[1] and Jochen Stutz[1]

Received 2 July 2006; revised 8 November 2006; accepted 21 February 2007; published 30 May 2007.

[1] Multiaxis differential optical absorption spectroscopy (MAX-DOAS) has many advantages that make it ideally suited for trace gas monitoring. MAX-DOAS instruments can be relatively small, are easy to operate, and allow long-term automated operation. The MAX-DOAS technique also allows derivation of vertical aerosol and trace gas profiles in the troposphere and thus the monitoring of pollution aloft. However, this relatively new technique still requires validation to determine uncertainties, for example, introduced by the radiative transfer modeling needed to derive trace gas concentrations. Here we present MAX-DOAS measurements of NO_2 and HCHO performed in the Gulf of Maine during the ICARTT campaign in summer 2004. O_4 measurements were performed to gain information on the vertical distribution of aerosols, which were used in radiative transfer calculations to convert the measured trace gas slant column densities to concentrations. The successful identification of an aerosol layer between 1 and 2 km altitude illustrates the potential for aerosol remote sensing. The comparison with LP DOAS measurements performed simultaneously shows that MAX-DOAS accurately measures trace gases that are well mixed within the boundary layer. MAX-DOAS measurements also provide valuable information on the vertical distribution of pollutants in and above the boundary layer, as demonstrated by the identification of elevated HCHO levels in a layer between 1 km and 2 km altitude. This phenomenon, which is associated with outflow of continental air from the American northeast, was not detected by in situ ground-based instruments.

Citation: Pikelnaya, O., S. C. Hurlock, S. Trick, and J. Stutz (2007), Intercomparison of multiaxis and long-path differential optical absorption spectroscopy measurements in the marine boundary layer, *J. Geophys. Res.*, *112*, D10S01, doi:10.1029/2006JD007727.

1. Introduction

[2] Absorption spectroscopy using scattered solar light has made significant contributions to our understanding of the stratospheric chemistry of O_3, BrO, OClO, and NO_2 [e.g., *Mount et al.*, 1987; *Noxon*, 1975; *Solomon et al.*, 1987; *Sanders et al.*, 1988]. Recently this method has been further developed to study tropospheric trace gases. This new multiaxis differential optical absorption spectroscopy (MAX-DOAS) technique is based on path integrated absorption measurements in different viewing directions, i.e., different elevation and/or azimuth angles [*Hönninger and Platt*, 2002]. The measured trace gas slant column density (SCD) is then converted to a vertical column density (VCD) using the air mass factor (AMF), i.e., the averaged light path enhancement for solar light traveling through the atmosphere compared to a straight vertical path [*Perliski and Solomon*, 1993]:

$$VCD = \frac{SCD}{AMF} \tag{1}$$

[3] For a tropospheric absorber, the AMF will strongly depend on the telescope's elevation angle α, while the stratospheric AMF will mainly depend on the solar zenith angle, ϑ. To a first approximation, which is based on the assumption that the tropospheric trace gas is located below the most probable scattering altitude of sunlight, ~5 km altitude, tropospheric and stratospheric air mass factors are simple geometric functions of α and ϑ [*Hönninger*, 2002]:

$$AMF_{Trop} = \frac{1}{\sin\alpha} \tag{2a}$$

$$AMF_{Strat} = \frac{1}{\cos\vartheta} \tag{2b}$$

[4] By measuring scattered light in the zenith and at a small elevation angle simultaneously, MAX-DOAS is thus able to distinguish between stratospheric and tropospheric absorbers. The comparison of low elevation and zenith absorption measurements also serves the purpose of removing Fraunhofer absorption lines in the solar spectrum. MAX-DOAS measurements therefore result in differential slant column densities (DSCD), i.e., the

[1]Department of Atmospheric and Oceanic Sciences, University of California, Los Angeles, California, USA.

0148-0227/07/2006JD007727$09.00

difference between low elevation and zenith SCDs [*Hönninger et al.*, 2004a]:

$$DSCD = SCD(\alpha) - SCD_{zenith} \quad (3)$$

[5] To interpret DSCDs a differential air mass factor (DAMF) must be calculated, which can then be used to determine the vertical trace gas column in the lower troposphere, VCD_{trop}:

$$DAMF = AMF(\alpha) - AMF_{zenith} \quad (4)$$

$$VCD_{trop} = \frac{DSCD}{DAMF} \quad (5)$$

[6] MAX-DOAS has been used to detect tropospheric BrO and OClO during the polar sunrise in the Arctic [*Miller et al.*, 1997; *Hönninger and Platt*, 2002], to determine tropospheric NO_3 profiles [*von Friedeburg et al.*, 2002], and for the measurement of pollutants such as NO_2 [*von Friedeburg et al.*, 2005; *Sinreich et al.*, 2005; *Leigh et al.*, 2006] and HCHO [*Heckel et al.*, 2005].

[7] MAX-DOAS has number of unique capabilities that make it ideally suited to monitor tropospheric trace gases. Clear identification of trace gases is achieved by using the unique differential absorption structure of each gas. Because the light paths are in the open atmosphere, calibrations are not necessary to derive DSCDs. At low elevation viewing angles light paths in the troposphere are long, and accordingly low detection limits can be achieved. MAX-DOAS instruments can be relatively small, simple to operate, and fully automated long-term operation is easily achievable. MAX-DOAS also offers the capability to determine trace gas concentrations averaged over the lowest 0.1–2 km of the atmosphere. Information on the vertical profiles of trace gases and optical properties of the tropospheric aerosols can also be retrieved [*Hönninger et al.*, 2004a, 2004b; *Wagner et al.*, 2004; *Friess et al*, 2006]. A particularly intriguing application of this capability is the identification and quantification of pollution above the boundary layer, as is for example often observed during pollution outflow from the east coast of the US over the Atlantic ocean [*Angevine et al.*, 1996a, 2004].

[8] The challenge in the application of MAX-DOAS is the conversion of the DSCDs to VCDs and vertical concentration profiles. Radiative transfer calculations are required to accurately determine the air mass factors (AMF). The uncertainties of both aerosol profile and trace gas profile introduce uncertainties in the AMF, which make it often difficult to assess the accuracy of MAX-DOAS results.

[9] MAX-DOAS is a relatively new method. Hence questions on the accuracy of tropospheric trace gas concentrations determined by MAX-DOAS and the suitability of MAX-DOAS observations for trace gas monitoring remain. Consequently there is a pressing need for validations of MAX-DOAS observations. Few such efforts have been reported. *Hönninger et al.* [2004b] compared long-path (LP)-DOAS observations made along a light path 30 m above the ice surface at Hudson Bay, Canada with MAX-DOAS observations of BrO at a 5° elevation viewing angle. Assuming a 1 km high mixed layer (based on previous observations) both instruments agreed well on most days. On a few days, however, only MAX-DOAS detected BrO. The authors suggest the presence of BrO in the free troposphere as a possible explanation. Observation of traffic-related NO_2 during the Bundesautobahn II motorway campaign in Heidelberg, Germany [*von Friedeburg et al.*, 2005], also allowed a comparison between LP-DOAS and MAX-DOAS data. The authors found reasonable agreement, considering the highly nonuniform conditions in this setup. *Heckel et al.* [2005], compared formaldehyde measurements in the Po Valley, Italy, by a Hantzsch-type in situ instrument, a long-path LP-DOAS, and a MAX-DOAS instrument. Under the assumption of a 500 m high well-mixed boundary layer the three instruments agreed in general within ±1 ppb, showing a very good agreement in the temporal behavior of HCHO.

[10] Validation of the MAX-DOAS method, which provides spatially averaged concentrations of tropospheric trace gases with in situ methods is often challenging if trace gases are not spatially homogeneously distributed. One way to overcome this challenge is to perform validation efforts downwind from trace gas sources, where a certain spatial homogeneity can be expected.

[11] In addition, LP-DOAS measurements are ideally suited to be compared to MAX-DOAS observations. LP-DOAS is a well-established method which provides concentrations averaged over a distance of a few kilometers. Depending on the light-path geometry, i.e., path length and altitude interval, LP-DOAS measurements observe a similar tropospheric volume as a MAX-DOAS instrument.

[12] Here we present results from colocated ground-based MAX-DOAS and LP-DOAS measurements of formaldehyde and nitrogen dioxide during the International Consortium for Atmospheric Research on Transport and Transformation (ICARTT, http://www.esrl.noaa.gov/csd/ICARTT/) study in summer 2004. The purpose of our study was to explore the capabilities of MAX-DOAS to accurately measure trace gas concentrations near the ocean surface and to determine if aerosol and trace gas profiles can be derived in this complex environment. We discuss the derivation of aerosol and trace gas profiles based on our MAX-DOAS observations. The results of this retrieval are then compared to the LP-DOAS measurements to assess the performance of the MAX-DOAS technique.

2. Experimental Section

[13] Simultaneous DOAS measurements were performed by UCLA's MultiAxis (MAX) DOAS and long-path (LP) instruments from 5 July through 10 August 2004 at the Isles of Shoals. The Isles of Shoals are a group of small islands located in the Gulf of Maine 10 km off the coast of Portsmouth, New Hampshire, USA (42°/58′N–70°/37′W). Levels of pollutants in the Gulf of Maine are strongly influenced by the unique meteorological conditions of this region [*Angevine et al.*, 1996a, 1996b, 2004]. Under southerly winds the Isles of Shoals are in the outflow of the New York–Boston corridor, receiving high levels of primary and secondary pollutants. Westerly winds lead to a more continental outflow which is dominated by biogenic emissions from the forested areas in New Hampshire and Maine. Only

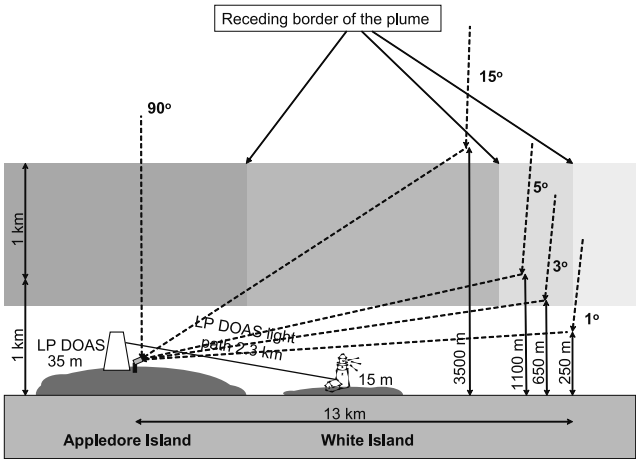

Figure 1. Experimental setup at the Isles of Shoals. Dashed lines indicate the MAX-DOAS viewing geometry (see text for more details). The LP-DOAS light path is shown as a solid line. This sketch is not to scale.

during easterly winds are marine, and thus relatively clean air masses observed.

[14] Previous observations during the North Atlantic Regional Experiment (NARE) [*Angevine et al.*, 1996a, 1996b] and the New England Air Quality Study (NEAQS) [*Angevine et al.*, 2004] often showed strong surface inversions and layering in the lowest 3 km of the atmosphere over the Gulf of Maine. Two different pollution transport scenarios can be observed. In the first case, continental air moves over the colder water of the Gulf of Maine and strong horizontal wind shear and a low-level jet lead to the formation of isolated atmospheric levels. In this case the air in the marine boundary layer has the composition of polluted continental air. In the more complex second case, continental air meets a sea breeze and, instead of being mixed with marine air, it is lifted to higher altitudes, while air at the surface remains unaffected by the continental outflow and relatively clean [*Angevine et al.*, 1996a]. A small amount of local emissions by recreational and commercial marine vessels is also present around the Isles of Shoals.

2.1. Long-Path (LP) DOAS Instrument

[15] The UCLA LP-DOAS system consists of a coaxial double Newtonian telescope which sends a collimated beam of light from a Xe-arc lamp onto a distant array of quartz corner cube prisms. This retroreflector array sends the light back to the telescope where it is focused onto a quartz fiber and sent to a grating spectrometer (Acton Spectra Pro 500), thermally stabilized to 35°C, with a photodiode array detector (Hoffmann Messtechnik with Hamamatsu S3904 PDA), cooled to −20°C. A detailed description of the LP-DOAS setup is given by *Alicke et al.* [2002] and *Stutz and Platt* [1997]. The LP-DOAS telescope was located on the 5th floor of a WWII observation tower on Appledore Island, 35 m above the ocean surface (Figure 1). The retroreflector array, determining the other end of the light path, was placed on White Island, 2.3 km south of the telescope and ∼15 m above the ocean surface. Four different wavelength intervals were measured sequentially. Here we report the measurements of NO_2 and HCHO made in the UV from 300 to 380 nm. Measurements in this interval were typically performed using the multichannel scanning technique [*Brauers et al.*, 1995] every 20–30 min with integration times of 5–10 min depending on visibility.

2.2. MAX-DOAS Instrument Description

[16] The UCLA MAX-DOAS instrument was developed for long-term automated observations of HCHO, NO_2, BrO, IO, OIO, and I_2. It consists of a telescope module with two elliptical 45° flat mirrors. One of the mirrors is mounted on a stepper motor to scan in the elevation plane. This mirror-motor combination is mounted on a rotating stage together with the second 45° mirror to scan the in the azimuth direction (Figure 2). This set up allows the instrument to point and collect light from any direction in the sky at any elevation except for a small interval of about 20° in the azimuth. Mounted between the rotating stage and a third 45° mirror that directs light onto a 150 mm focal length lens is a filter wheel driven by another stepper motor. The filter wheel is used to block the light beam to measure background spectra. The lens focuses the light onto a 5 m long, 1 mm diameter quartz fiber that transmits the light to the 200 μm width entrance slit of an Czerny-Turner type grating spectrometer (Acton Spectra Pro 300i, 600g/mm grating) coupled to a Hamamatsu 1024 pixels photodiode array (Hoffmann Messtechnik with Hamamatsu S3904 PDA). The spectrometer has a spectral resolution of 0.92 nm which

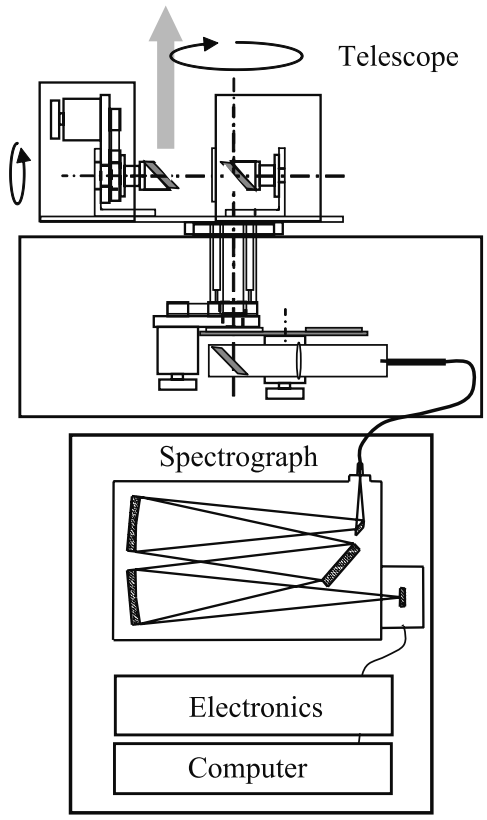

Figure 2. Sketch of the UCLA MAX-DOAS instrument. The telescope assembly, the spectrograph, electronics, and the computer are mounted in two weatherproof enclosures.

Table 1. DOAS Trace Gases Spectral Evaluation Information[a]

Trace Gas	Wavelength Interval, nm	Trace Gas References Fitted
NO_2	413–446	NO_2, O_4, IO, H_2O, $C_2H_2O_2$
HCHO	328–346	HCHO, NO_2, O_4, BrO, O_3
O_4	350–389	O_4, NO_2, HCHO, BrO, O_3

[a]The spectral intervals were chosen to minimize residual structures and to optimize the stability of the fit.

is calculated as the full width at half of the maximum of the mercury spectrum line at 345 nm, and a linear dispersion of 0.13 nm/pixel. It is thermally stabilized at 35°C. The PDA is cooled to −20°C. The stepper motors, spectrometer heating, PDA cooling, signal processing and data transfer are controlled by a personal computer. The telescope assembly has an angular field of view of ∼0.4°. The pointing accuracy is ±0.075° in elevation and ±0.15° in azimuth. Particular care is given to the precise leveling to within ±0.06° of the telescope to ensure the accuracy of the scanning elevation angles. The instrument automatically records Hg emission line spectra, dark current, and electronic offset spectra at night.

[17] On Appledore Island the MAX-DOAS instrument was located at the bottom of the WWII tower and was collecting scattered sunlight from five different elevation viewing angles: 1°, 3°, 5°, 15°, and 90°; with an azimuth viewing angle almost parallel to the LP-DOAS line of sight (Figure 1). The MAX-DOAS instrument was measuring in subsequent sets of elevation viewing angles in a 130 nm wavelength interval with a center wavelength of 385 nm. A typical sequence for one wavelength interval required approximately 5 min.

2.3. Spectral Evaluation

[18] The spectral analysis of the LP and MAX-DOAS spectra was performed using a combination of linear and nonlinear least squares fit [*Stutz and Platt*, 1996]. Details of the LP-DOAS evaluation procedure are given by *Alicke et al.* [2002] and will not be repeated here. The absorption cross sections used in the LP-DOAS analysis are identical to those used for the MAX-DOAS analysis (see below).

[19] MAX-DOAS spectra were analyzed in three different spectral intervals (Table 1). In all three intervals a temporally close zenith spectrum (as a Fraunhofer reference) and simulated Ring spectrum [*Vountas et al.*, 1998] were fitted together with a polynomial of degree 5 after being low-pass filtered by a ten fold triangular smoothing.

[20] All reference absorption cross sections were convoluted with a instrument function determined using a measured Hg line. The convolution process also corrected for the I_0 effect, caused by the highly structured solar spectrum [*Aliwell et al.*, 2002]. Table 2 lists the references for the absorption cross sections used in the analysis. Figure 3 shows an example of the spectral evaluation of HCHO for a MAX-DOAS spectrum recorded on 17 July 2004 at 1852 UT at a 1° elevation viewing angle.

[21] In the presence of thick fog, when solar radiation is direction-independent, peak-to-peak residual values were $2 - 3 \times 10^{-4}$. This value represents the instrument-imposed limit on optical density that can be detected in a time interval of 1–2 min. During sunny days with high trace gas concentrations average peak-to-peak residual values for the MAX-DOAS instrument were in the range of 9×10^{-4} to 1.2×10^{-3}. The higher residual in this case arises from uncertainties in the description of the absorption structures. The DSCD error averaged over the campaign for HCHO was 1.1×10^{16} molecules/cm^2 and 5.0×10^{14} molecules/cm^2 for NO_2.

2.4. Radiative Transfer Calculations

[22] In order to interpret the MAX-DOAS absorption measurements, radiative transfer calculations were performed using the TRACY model developed at the University of Heidelberg, Germany [*von Friedeburg*, 2003]. This 3-D Monte Carlo radiative transfer model was designed for the interpretation of MAX-DOAS slant column densities, and derives air mass factors for trace gas profiles at a given wavelength, observation geometry, and aerosol load. All air mass factors were calculated for spatial location and the solar zenith and solar azimuth at the time of the measurement.

[23] For the most simple retrieval example, concentration of a trace gas that is confined to and evenly distributed within the boundary layer can be calculated on the basis of the DSCD measured by the MAX-DOAS instrument using equations (3)–(5). The AMF for this case is calculated by TRACY, on the basis of a user defined aerosol profile. The conversion from the tropospheric VCD to a concentration can then be derived using the boundary layer height. However, in many cases the aerosol profiles, which have a large impact on the AMFs, are unknown, and trace gases are often not evenly distributed in the boundary layer. In this case the VCD and concentration retrieval is more involved.

[24] Random errors in AMF calculations from TRACY have their origin in the statistical errors of the Monte Carlo method, i.e., the statistics of averaging over a number of modeled photons. Because of limits in computer time, this error was on the order of 2%. It should be noted that the error can be further reduced by using a larger number of photons.

2.5. Derivation of Aerosol Profiles

[25] Because radiative transfer in the atmosphere is strongly influenced by aerosol scattering, accurate informa-

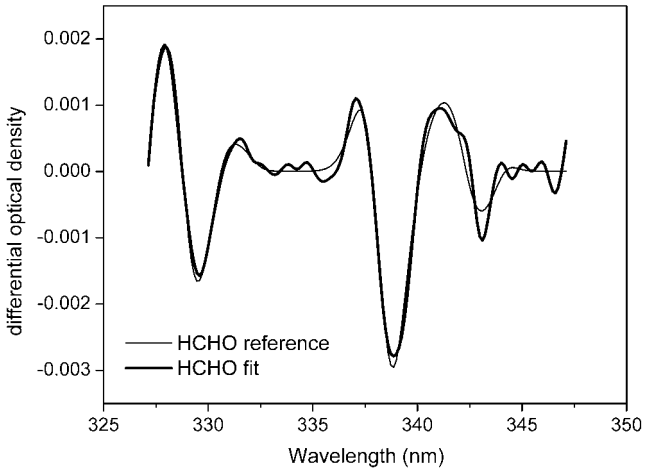

Figure 3. Result of the HCHO spectral analysis of a 1° elevation viewing angle MAX-DOAS spectrum recorded on 17 July 2004 at 1853 UT. A HCHO DSCD of $(1.32 \pm 0.08) \times 10^{17}$ molecules/cm^2 was found in the spectrum. For a 700 m high well-mixed boundary layer this is equivalent to a mixing ratio of 4.9 ± 0.5 ppb.

Table 2. References Used for DOAS Analysis

Spectral Reference	Source
NO_2	reference cell recorded by the instrument at the measurements wavelength interval calibrated with NO_2 absorption cross section reference by *Voigt et al.* [2002]
O_4	*Greenblatt et al.* [1990]
HCHO	*Meller and Moorgat* [2000]
IO	*Hönninger* [1999]
H_2O	HITRAN, 2004
$C_2H_2O_2$	*Volkamer et al.* [2005]
O_3	*Voigt et al.* [2001]
BrO	*Wahner et al.* [1988]

tion on the vertical profiles of aerosol extinction coefficient, single scattering albedo, and phase function is required. Our investigation, as well as previous studies [e.g., *von Friedeburg*, 2003; *Wittrock et al.*, 2003; *Heckel et al.*, 2005] show that aerosol extinction profiles have the strongest impact on AMF values.

[26] By measuring the UV/visible absorption features of O_4, the collisional complex of two oxygen molecules, MAX-DOAS offers an elegant way to obtain the required aerosol data [*Wagner et al.*, 2004]. The atmospheric O_4 concentration is solely dependent on the square of the air pressure, and therefore its concentration profile is to a very good approximation constant with time, with largest values in the lower atmosphere. Consequently, the O_4 DSCDs measured by the MAX-DOAS depend solely on the AMF, hence on radiative transfer. The best aerosol profile for the scenario under investigation is found when the measured O_4 DSCD, divided by the modeled O_4 DAMFs, yield the same values for the O_4 VCD for all elevation angles.

[27] In a recent theoretical study *Friess et al.* [2006] describe how the use of O_4 absorption bands at four wavelengths together with MAX-DOAS intensity data can be used for an automated aerosol retrieval.

[28] Here we adopted a different approach, by using back trajectories (from NOAA ARL HYSPLIT model http://www.arl.noaa.gov/ready/hysplit4.html) and wind profiler data (from the Environmental Technology Laboratory Boundary Layer Wind Profiler Studies, NOAA Environmental Technology Laboratory) to constrain the shape of aerosol profiles by providing boundary layer heights, and the air mass origin at various altitudes. The various aerosol profiles in this study are variations of standard aerosol profiles used in the radiative transfer modeling comparison exercise by *Hendrick et al.* [2006], constructed for maritime, rural, and urban scenarios according to the model of *Shettle* [1989]. All profiles, with the exception of two profiles used for a sensitivity study, are based on a single scattering albedo of (0.982). The phase function is based on *Henyey and Greenstein* [1941].

[29] On the basis of the meteorological data, we constructed aerosol profiles and compared the tropospheric O_4 VCDs of the four low elevation scans. The profiles were then manually optimized within the boundary conditions imposed by the meteorological observations. The result of this process and the detailed explanation of the aerosol extinction profiles (Figure 4) will be given below.

[30] The aerosol extinction profile that described the O_4 VCDs best was then used as input to calculate DAMFs for the target species. The optimization was done manually in our study. This was motivated by a desire to better understand how MAX-DOAS measurements are influenced by meteorological conditions and the vertical aerosol and trace gas distribution, as well as to explore the potential of an automated retrieval when applied to real data.

2.6. Concentration Profile Retrieval

[31] In addition to the dependence on the aerosol profile, trace gas AMFs are also a function of the vertical trace gas concentration profile itself. This can be illustrated by introducing Box-AMFs, or BAMFs, which are defined as the air mass factors for a given atmospheric layer. By subtracting the zenith sky BAMF from the low elevation viewing angle BAMF in the respective layer we obtain Differential Box AMFs (DBAMFs).

[32] Figure 5 shows examples for the aerosol scenarios "Trop" and "Trop9" (see Figure 4) derived for July 2004 at Appledore Island. The lowest part of the boundary layer has a high DBAMF of ~40 for the 1° elevation viewing angle, while the 15° DBAMF is only ~3.5. Trace gases at higher altitudes contribute more evenly to the AMF of different viewing elevation angles.

[33] Differential Box AMFs along with the MAX-DOAS measured DSCDs were used to retrieve trace gas profiles for

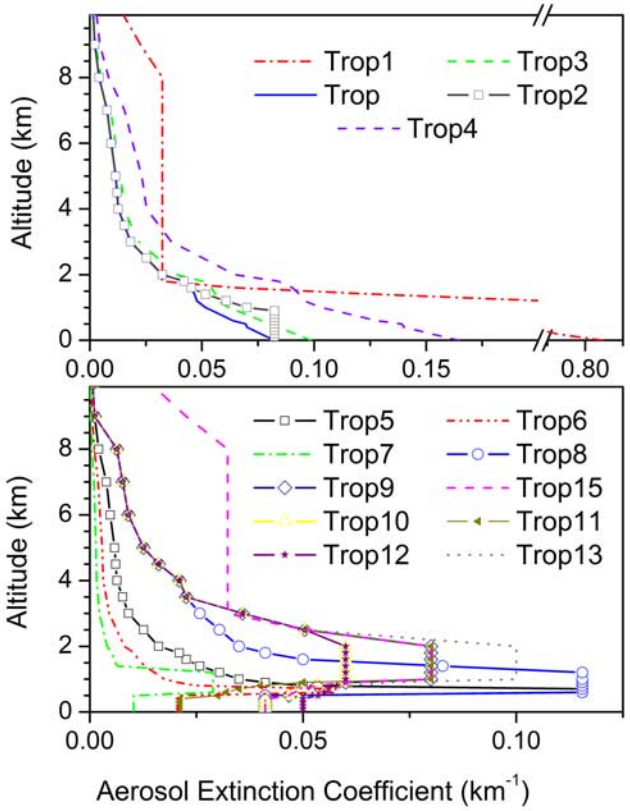

Figure 4. Aerosol extinction coefficient profiles used as input for the radiative transfer model. (top) Profiles with the maximum extinction at the surface and (bottom) profiles with elevated extinction aloft.

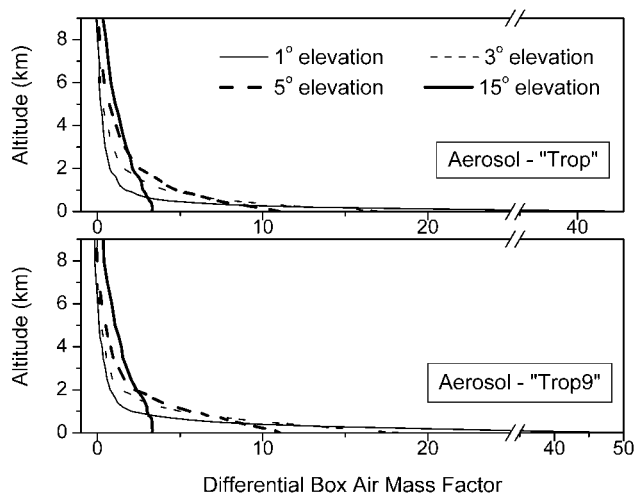

Figure 5. Differential box AMF at 422 nm for the "Trop" and "Trop9" aerosol profiles (see Figure 4) at a solar zenith angle of 24.8.

Appledore Island. A DSCD for a particular elevation viewing angle, α_i, can be expressed as:

$$DSCD(\alpha_i) = \sum_{j=1}^{m} \left[DBAMF_{ij} \cdot \Delta h_j \cdot C_j \right] \quad (6)$$

[34] Where i is the index of the elevation viewing angle, j is index of modeled atmospheric altitude interval with height Δh_j, C_j is concentration of the trace gas within the jth box, and $DBAMF_{ij}$ is the differential box air mass factor for elevation α_i and altitude j.

[35] To derive a trace gas profile we started with an initial trace gas vertical profile, constrained by meteorological observations, and calculated the DSCDs for each elevation viewing angle using equation (6). These calculated DSCDs were then compared with the DSCDs measured by the MAX-DOAS. The trace gas vertical concentration profile was then iteratively adjusted until agreement between calculated and measured DSCDs was achieved for all elevation viewing angles. Details of this manual optimization process are given below.

3. Results and Discussions

[36] We chose two days of our MAX-DOAS measurements, 11 and 17 July 2004, for our intercomparison. Both days were cloud-free, simplifying the MAX-DOAS retrieval. Wind trajectories show that the sampled air masses came from approximately the same direction. At the same time NO_2 and HCHO levels measured by the LP-DOAS as well as DSCDs from the MAX-DOAS differ significantly between these two days. The days 11 and 17 July 2004 are therefore ideally suited to study the accuracy of MAX-DOAS measurements. In the following, the derivation of aerosol profiles will be discussed, followed by the intercomparison of NO_2 and HCHO measurements between MAX-DOAS and LP-DOAS.

3.1. Derivation of Aerosol Properties

[37] Following the approach discussed above, various aerosol extinction profiles (Figure 4, top) were applied to determine the conditions at Appledore Island on 17 July 2004. Figure 6 shows the O_4 VCD calculated on the basis of the MAX-DOAS observations from 17 July 2004 at 1500 UT for the aerosol profiles shown in Figure 4. Very high aerosol extinctions ("Trop1," Figure 4) lead to different VCDs for all elevation viewing angles, and to unreasonably high VCD values. Decreasing the extinction coefficients at the ground ("Trop4" and "Trop3," Figure 4) still overestimates the DVCDs for 1°, 3°, and 5° elevation viewing angles (Figure 6), but improves the agreement successively. The best aerosol profile for 17 July, "Trop" in Figure 4, has an extinction coefficient at the ground of 0.08 km^{-1}, which decreased linearly in the lowest 2 km and exponentially in the rest of the troposphere. This profile leads to the expected value of the O_4 VCD and to an excellent agreement between the four elevation angles. A profile with constant aerosol extinction of 0.08 km^{-1} in the lowest kilometer and an exponential decay aloft ("Trop2") showed larger differences in the VCDs.

[38] The entire data set of MAX-DOAS measured O_4 DSCDs and VCDs derived with the "Trop" profile on 17 July 2004 is shown in Figure 7. In general, the agreement between the VCDs from the four elevation viewing elevation angles is very good, except between 1700 UT and 2000 UT. We attribute this disagreement to a change in the actual aerosol profile during this time.

[39] In the same way as for 17 July 2004, all aerosol profiles depicted in Figure 4 were used to identify those that best describe the conditions at Appledore Island on 11 July 2004 (Figure 8). The O_4 VCDs of profiles Trop3, Trop2, and Trop (Figure 4), of which Trop agrees best, allow a first estimate of the magnitude of the extinction profile. However, the O_4 VCDs at 1° elevation viewing angle was consistently low for all these profiles. Because the 1° elevation angle measurement is most sensitive to the tropospheric layers closest to the surface (see Figure 5), the "true" aerosol extinction profile must have smaller aerosol extinction at the surface than aloft. To further constrain this aerosol profile we calculated HYSPLIT back trajectories for 1500 UT on 11 July 2004

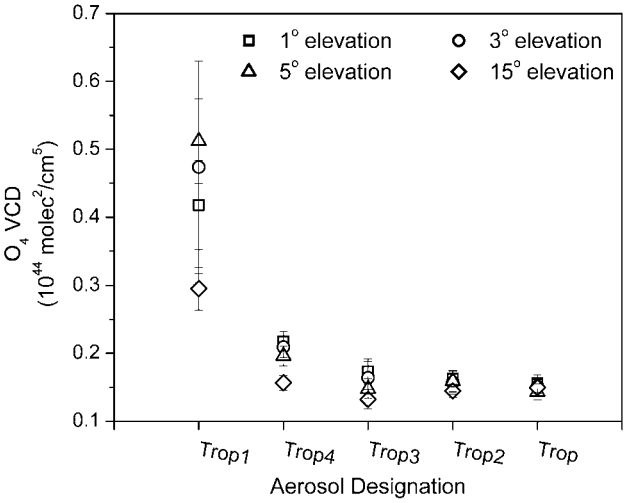

Figure 6. O_4 VCDs calculated on the basis of DSCDs observed on 17 July 2004, 1515 UT (SZA = 28.8), and various aerosol extinction profiles shown in Figure 4.

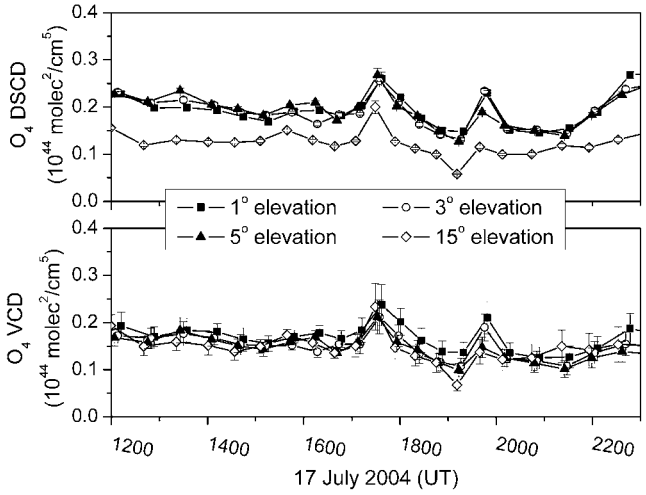

Figure 7. MAX-DOAS O_4 DSCDs and VCDs on 17 July 2004. The VCDs were derived on the basis of the "Trop" aerosol profile (Figure 4).

which showed a mixed layer height of approximately 300 m and different air mass origins below and above 300 m. NOAA ETL wind profiler data at Appledore Island showed sharp wind speed and wind direction changes around 300 m altitude, also pointing to a mixed layer boundary at this altitude. Between 300 m and 1000 m altitude the wind direction gradually changed. Between 1 km and 2 km the wind direction was fairly constant and changed again above 2 km. These changes in wind direction support the assumption that the aerosol extinction coefficient above 300 m is different from that at the surface. Another piece of evidence for a layer of aerosol comes from the MAX-DOAS measurements of HCHO. Formaldehyde DSCDs for 11 July 2004 were elevated but did not exhibit a dependence on the elevation viewing angle, suggesting that most of the HCHO was located aloft (see also discussion below). We therefore concluded that a layer of continental air with increased formaldehyde and high aerosol extinction was present above ~300 m. We consequently changed our original aerosol extinction profile to include such a layer of high aerosol extinction ("Trop5" through "Trop18," Figure 4 (bottom)). As illustrated in Figure 8 aerosol profiles "Trop8" and "Trop9" both produce a very good agreement in O_4 VCDs from all four elevation viewing angles. The fact that both profiles agreed well is most likely due to the agreement of the vertically integrated aerosol extinctions for both aerosol profiles, i.e., 0.232 for "Trop8" and 0.234 for "Trop9." Therefore we cannot with certainty determine which of these two profiles is the "true" profile for 11 July 2004 on the basis of the MAX-DOAS observations alone. However, wind profiler data points toward "Trop9" as a more accurate representation of the conditions during this day and time, since the sharp wind speed and direction change between 300 m and 400 m followed by the more gradual change between 400 m and 1 km observed by the wind profiler agrees better with aerosol extinction profile "Trop 9."

[40] We also calculated O_4 VCDs resulting from the aerosol extinction profile "Trop15" that has higher extinction coefficients than "Trop9" above 2.5 km. For this modified aerosol, O_4 VCDs also agree for all elevation viewing angles. This is not surprising because the box air mass factors for the zenith and low elevation viewing directions are very similar in this altitude range. Since MAX-DOAS analysis for the low elevation viewing angles is performed relative to the 90° viewing direction, little information on the tropospheric layers above 3 km is left in the O_4 DSCDs.

[41] The effect of aerosol composition on the O_4 VCDs was also investigated. Radiative transfer calculations for the "Trop9" profile were performed with the single scattering albedo value of (0.982) for marine aerosol. In addition, we performed calculations for aerosol that had the same vertical extinction profile as "Trop9," but the aerosol layer aloft was assigned a single scattering albedo values of 0.95 for rural aerosol ("Trop18"), and 0.7 for urban aerosol ("Trop16") [*Shettle*, 1989]. These changes did not make a significant impact on the agreement between O_4 VCDs.

[42] Figure 9 shows MAX-DOAS measured O_4 DSCDs as well as VCDs calculated with the "Trop9" aerosol profile. Between 1500 UT and 1800 UT a very good agreement between the O_4 VCDs of the four elevation angles is observed, showing the presence of the elevated aerosol layer during this period.

[43] The examples presented here show clearly that MAX-DOAS is able to determine the vertical distribution of aerosol in the lowest 2–3 km of the atmosphere. Various factors have to be considered to determine the uncertainty of the retrieval. The DOAS measurement and the spectral analysis of the O_4 absorption bands introduce a statistical error on the order of 4%. Another statistical uncertainty of 2% originates in the Monte Carlo RTM modeling of the O_4 and trace gas AMFs. The uncertainty most difficult to quantify results from ambiguities between two aerosol profiles yielding sets of O_4 DSCDs which match the observations within the uncertainties. We approached this problem by constraining the profiles with meteorological observations and by systematically testing different sets of aerosol profiles (for example, Figure 4). On the basis of the

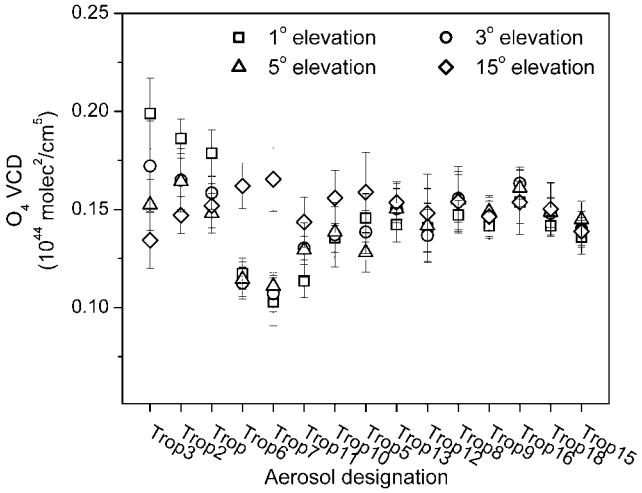

Figure 8. O_4 VCDs calculated on the basis of DSCDs observed on 11 July 2004, 1500 UT (SZA = 28.9), and various aerosol extinction profiles shown in Figure 4.

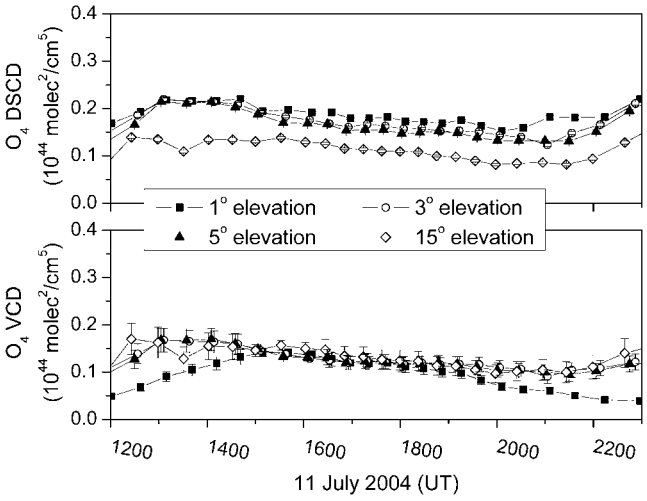

Figure 9. O_4 DSCDs and VCDs on 11 July 2004. The VCDs were derived on the basis of the "Trop9" aerosol profile (Figure 4).

comparison of the different O_4 VCD sets in this work, the aerosol extinction coefficient error can be estimated as 0.01 km^{-1}, i.e., ~12% at altitudes below ~4 km. The uncertainty in the height of the boundary layer and the elevated layer, determined on the basis of our calculations, is in the range of 100 m for the MBL and 200–300 m for the elevated layer.

[44] While the exact shape of the aerosol layer above the mixed layer is somewhat uncertain it is clear that MAX-DOAS is able to identify such layers, which often go unnoticed at the ground. As described by *Friess et al.* [2006] the aerosol retrieval can be improved and automated by measuring O_4 absorptions at more wavelengths and by including the intensity of the measurements. In our case, O_4 absorptions at one wavelength and additional meteorological information was sufficient to retrieve the profile successfully. It should be possible to automate this retrieval method in order to use MAX-DOAS as an aerosol monitoring tool, i.e., as an alternative to much more expensive and work intensive methods such as backscatter LIDAR or tethered balloons.

3.2. Trace Gases on 17 July 2004

[45] The DSCDs of HCHO on 17 July showed a clear separation in the four elevation angles (Figure 10). From the wind profiler data for 17 July 2004 at Appledore Island, a MBL height of 700 m was estimated. Because the Isles of Shoals are far from any HCHO or HCHO precursor source we assumed that formaldehyde was well mixed in the MBL. On the basis of the aerosol profile derived for this day ("Trop," Figure 4) we then calculated DBAMFs for formaldehyde well mixed within the lowest 700 ± 100 m. As shown in Figure 10, the MBL concentrations derived on the basis of this assumption before 1800 UT agree for all measured elevation viewing angles. A number of other profiles (not shown) were used to determine the uncertainty of these results. For example, tests with more than 1 ppb of HCHO above 700 m lead to DCSD values for the 15° viewing elevation angle higher than the observations. Above the 700 m boundary layer, we can therefore not detect HCHO levels below 1 ppb extending up to 4 km attitude. A lower or higher boundary layer leads to changes in the 3° and 5° elevation DSCDs, while higher or lower concentrations in the lowest 100 m above the ocean surface influence the 1° elevation DSCD. We therefore determined an error for the boundary layer height of ±100 m. Within the boundary layer the uncertainty in the derived HCHO concentrations is ±0.5 ppb for the elevation angles below 15°. The 15° error is higher because of the lower sensitivity toward the boundary layer.

[46] HCHO mixing ratios averaged over the MBL increased slowly from 2 ppb to 4 ppb from 1200 to 1800 UT. The HCHO concentrations after 1800 UT showed a certain dependence on elevation, which is not too surprising since the O_4 analysis in section 3.1 indicated that the aerosol profile changed around this time.

[47] A comparison with the simultaneous LP-DOAS data showed an excellent agreement, considering that the LP-DOAS measures in a shallow layer near the ocean surface, while the MAX-DOAS mixing ratios are averaged over the MBL. The two measurements in general agreed within 1 ppb and also showed a very similar temporal variation. It should be noted that, considering the errors of both measurements and the uncertainty in the boundary layer height of ~100 m, this agreement confirms our observation that HCHO is vertically well mixed in the MBL. *Angevine et al.* [2004] describe a case very similar to our observations where continental pollution was confined to a 400–600 m deep boundary layer at Appledore Island.

[48] The NO_2 DSCDs measured by the MAX-DOAS on 17 July 2004 also exhibit a clear separation between the elevation viewing angles (Figure 11), suggesting that NO_2, just as HCHO, must be well mixed within the boundary layer or at least confined close to the ocean surface. Using the same radiative transfer model parameters for NO_2 as for HCHO leads to NO_2 mixing ratios of ~1 ppb in the MBL

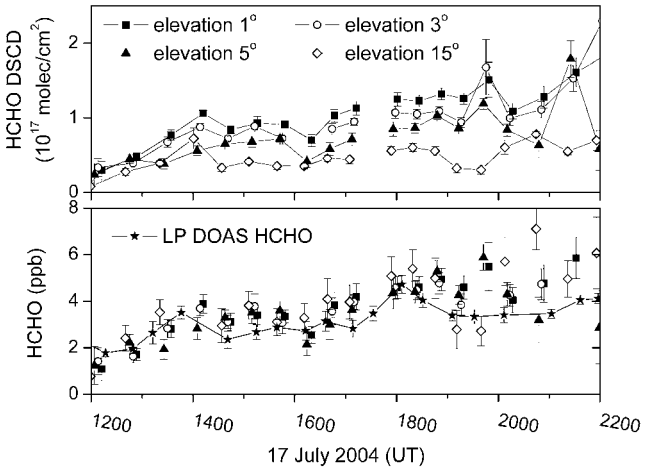

Figure 10. MAX-DOAS HCHO DSCDs and mixing ratios on 17 July 2004. Mixing ratios were calculated on the basis of the "Trop" aerosol profile and a 700 m high well-mixed boundary layer. The comparison with LP-DOAS observations shows a very good agreement between the two methods.

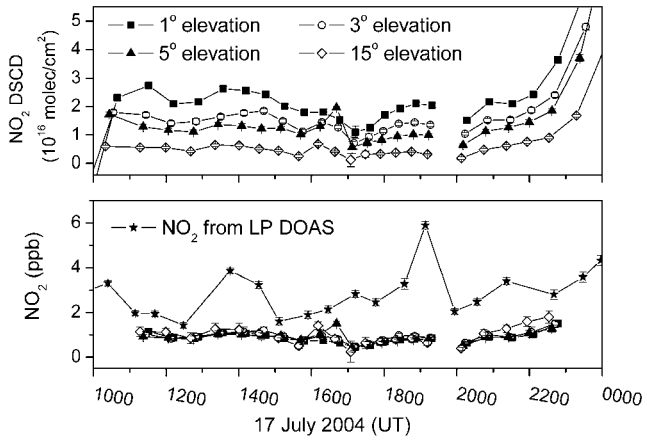

Figure 11. MAX-DOAS NO_2 DSCDs and mixing ratios on 17 July 2004. Mixing ratios were calculated on the basis of the ''Trop'' aerosol profile and a 700 m high, well-mixed boundary layer. The disagreement between MAX-DOAS and LP-DOAS observations is most likely due to a shallow layer of NO_2 above the ocean surface.

that show no dependence on the elevation angle before 1900 UT. The agreement between the four elevation viewing angles seems to suggest that the NO_2 in the MBL was also well mixed. However, LP-DOAS and MAX-DOAS nitrogen dioxide measurements on 17 July do not agree as well as those of formaldehyde. LP-DOAS NO_2 was in general 1–3 ppb higher and also showed a more pronounced temporal variability. The most likely explanation for this disagreement is a shallow layer of NO_2 from ship emissions in the stable MBL between the coast and Appledore Island. Because the LP-DOAS light beam is located in this layer it is very sensitive to NO_2 close to the ocean surface. The MAX–DOAS, on the other hand, is fairly insensitive to such a shallow pollution layer. Radiative transfer calculations confirm that a layer ~50 m high with 3 ppb of NO_2, as seen by the LP-DOAS, would not have detectable influence on the MAX-DOAS results. The uncertainty in the boundary layer averaged NO_2 mixing ratio is approximately ±0.2 ppb. Above 700 m altitude less than 0.1 ppb of NO_2 is present. As in the case of HCHO, the boundary layer height is known to within ±100 m.

[49] Our observations illustrate that care has to be taken in using MAX-DOAS measurements for the interpretations of other ground measurements. In particular in cases where fresh emissions accumulate close to the surface, MAX-DOAS will not probe the same air mass as ground-based in situ instruments.

[50] On the other hand, the MAX-DOAS data delivers an otherwise unobtainable piece of information, the NO_2 levels averaged over the lowest few hundred meters of the troposphere, an area which is otherwise difficult to probe. The combination of in situ ground measurements and the altitude averaged MAX-DOAS observations allows conclusions on the mixing of the boundary layer, which can be a valuable tool to assess how representative ground measurements are for the entire boundary layer.

3.3. Trace Gases on 11 July 2004

[51] Figure 12 shows formaldehyde DSCDs measured by MAX-DOAS on 11 July 2004. Surprisingly, the DSCDs do not exhibit a dependence on the elevation viewing angle in the morning, but are in the same range as those on 17 July. A first conclusion of this observation is that HCHO is located at a certain altitude above the ocean surface, as illustrated in Figure 4. DBAMFs calculated for the aerosol profile ''Trop9'' (Figure 5) were used by the method described in section 2.6 to derive a formaldehyde vertical concentration profile for 11 July 2004.

[52] Through systematic testing of a large number of HCHO vertical profiles we derived a profile for which the DSCDs calculated from the profiles according to equation (6) agreed with the measured DSCDs. Tested profiles were created on the basis of a combination of meteorological information and an understanding of how different altitudes affect the DSCDs for different elevation viewing angles.

[53] While we cannot show all profiles tested in our optimization procedure, we will illustrate the dependence of the DSCDs on the profile using a selection of example profiles (Figure 13). To confirm our first conclusion that HCHO is elevated aloft we used a fairly uniform profile in the lowest 3 km of the atmosphere (profile 5, Figure 13), which shows a distinct disagreement at the lower elevation DSCDs. A profile that only contained HCHO between 1 and 2 km altitude (profile 15, Figure 13) leads to the 5° and 1° DSCDs being too high and too low, respectively. To increase the value of the 1° DSCD, we added HCHO in the lower part of the profile (profiles 18, 19 and 20, Figure 13). Finally HCHO was added above 2 km altitude, assuming an exponential decay with height (profile 12, Figure 13). The optimum profile (profile 12, Figure 13) thus has a low HCHO mixing ratio at the surface of ~0.5 ppb ± 0.5 ppb, which is consistent with the LP-DOAS measurements (Figure 12). A high formaldehyde mixing ratio of 3.6 ± 0.7 ppb is found between 1 km and 2 km altitude, which is within the layer of high aerosol extinction discussed above. The HCHO levels then decrease exponentially above 2 km.

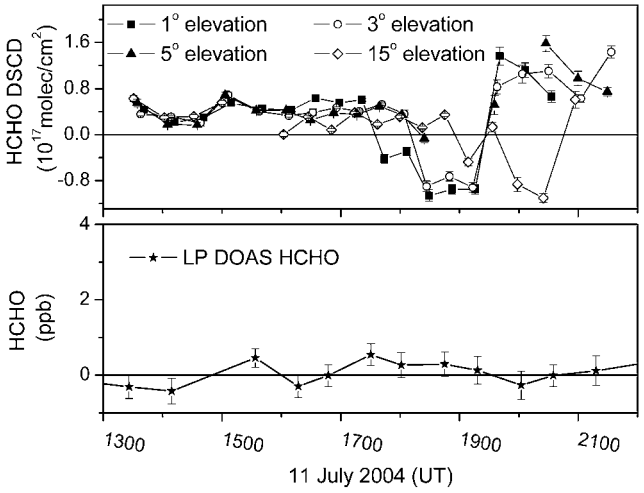

Figure 12. MAX-DOAS DSCDs and LP-DOAS mixing ratios of HCHO on 11 July 2004.

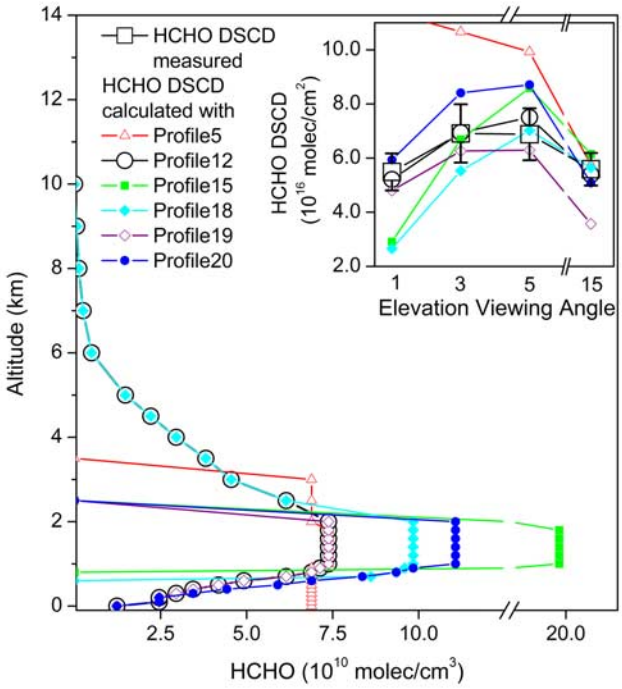

Figure 13. HCHO vertical concentration profile used in the analysis of the MAX-DOAS observations on 11 July 2004, 1500 UT. The black line with open circles shows the HCHO vertical concentration profile that fits the observations best (profile 12). Other lines show other HCHO vertical profiles used in the retrieval. The insert compares the HCHO DSCDs calculated on the basis of the various profiles with the observations by the MAX-DOAS instrument.

[54] The formaldehyde concentrations in the pollution layer are similar to the levels measured in the MBL on 17 July. Formaldehyde at Appledore Island originates from the photochemical degradation of continental organic precursors. Because biogenic emission, for example of isoprene, are important in the New England area [*Palmer et al.*, 2003], continental air masses often contain elevated levels of formaldehyde in the Gulf of Maine, even in the absence of a large anthropogenic influence (see below). Consequently it is not surprising that the maximum HCHO levels on the two example days are similar. An explanation for the observed aerosol and HCHO layer can be found in the particular meteorology around Appledore Island. The Gulf of Maine is known for a shallow, and stable, marine boundary layer over which continental air is lifted and transported [*Angevine et al.*, 1996a]. Under these conditions, in situ measurements techniques at the surface will not detect the pollution transport aloft. MAX-DOAS, however, successfully detects these events.

[55] Between 1745 and 1930 UT negative HCHO DSCD were observed by the MAX-DOAS. First, the 1° elevation angle signal becomes negative, followed sequentially by the 3°, 5°, and 15°. After excluding instrumental problems as an explanation for these observations, we concluded that this peculiar event was caused by changes in the meteorological conditions in and around Appledore Island in combination with the particular viewing geometry of the MAX-DOAS.

[56] As illustrated in Figure 1 the observations at different viewing elevation angles are not only sensitive to the vertical distribution of trace gases, as explained in section 2.6, but in some cases also to horizontal gradients. Using a description based on the modeled average or most likely light path for a certain elevation angle it is possible to gain a better understanding of the complex radiative transfer. The light path close to the telescope is predominantly determined by geometry, i.e., equation (2a). The length of this "geometric path," i.e., distance from the telescope, is determined by the last scattering event before the light enters the telescope. The average distance and height of the last scattering events can be determined by TRACY as the average of these events over all simulated photon paths. Please note that we will refer to the average value to simplify the discussion. For our 11 July case the 1°, 3°, 5°, 15° and 90° final altitudes of the "geometric paths" are at 250 m, 650 m, 1100 m, 3500 m, and 5700 m respectively. The horizontal distance between the telescope and the last scattering event is ~13 km for the all low elevation observations and 0 km for the zenith observation. Beyond the "last" scattering altitude and up to an altitude of 4750 m, 5203 m, 5189 m, 6600 m, and 7200 m, respectively, single or multiple scattering of sunlight occurs. It is difficult to define a light path in this "scattering" layer, since the intensity along the viewing geometry of the MAX-DOAS is determined by the statistics of the scattering events. However, it is qualitatively clear that the horizontal distance from the telescope at which light passes through this layer increases for decreasing elevation viewing angles.

[57] The MAX-DOAS approach is based on the comparison of zenith and low elevation angle observations. To use this technique for vertical profiling, assumptions on the horizontal uniformity of the trace gas concentrations have to be made. Such a case where we believe this condition was met was described above. If, however, this condition is not

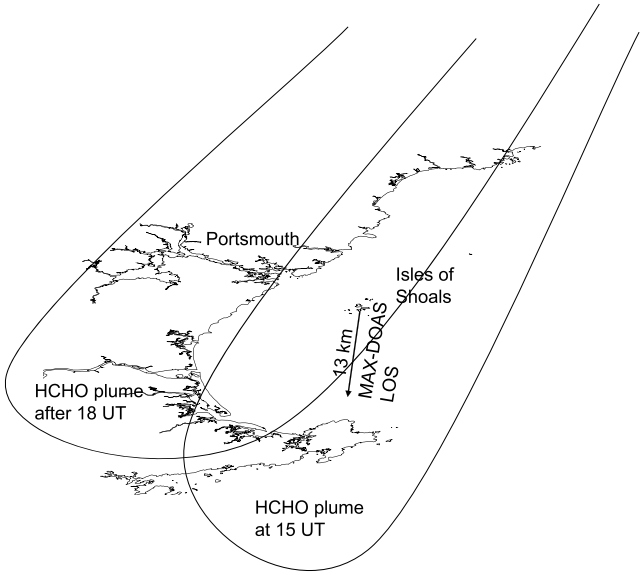

Figure 14. Proposed temporal evolution of the HCHO plume over the Gulf of Maine explaining the negative DSCDs observed between 1745 UT and 1930 UT on 11 July 2004.

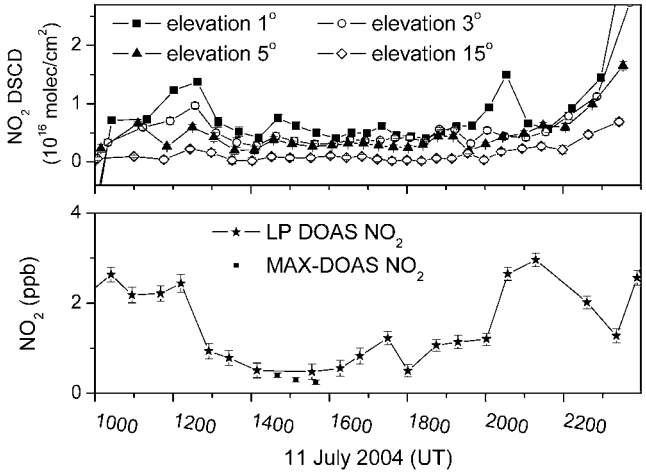

Figure 15. MAX-DOAS DSCDs and LP-DOAS mixing ratios of NO_2 on 11 July 2004. MAX-DOAS DSCDs and LP-DOAS mixing ratios of NO2 on 11 July 2004. The derivation of the MAX-DOAS concentrations shown in the bottom plot are discussed in the text.

met, challenges arise in the interpretation of MAX-DOAS observations. We believe that we observed an extreme horizontal concentration gradient between the location of the instrument, and therefore the air mass probed by the zenith scan, and the location where sunlight passes through the "scattering layer," i.e., where low elevation angles probe the atmosphere above 500 m.

[58] At 1500 UT the direction of the north-northeasterly wind observed by the radar wind-profiler at all altitudes is near-parallel to the MAX DOAS viewing geometry. Conditions such as this alleviate problems of spatial inhomogeneity, and we observed a fairly uniform HCHO plume between 1 km and 2 km altitude, which was located above all parts of the MAX-DOAS line of sight. These conditions allowed the determination of the vertical profile shown in Figure 13. Between 1530 and 1730 UT, however, the wind direction between 1 km and 2 km turned easterly (see Figure 14). This leads to a situation where the plume is still present above Appledore Island while it has drifted away from parts of the lines of sight of the low elevation scans (Figure 14). As a consequence the zenith scan at 1745 UT probes the HCHO plume, while the 1° elevation scan, which probes the 1–2 km altitude range in ~13 km distance, does not observe the plume anymore. A comparison of the zenith scan with the low elevation scan, as performed by the MAX-DOAS analysis, now leads to the negative 1° DSCDs. It is interesting to note that a spectroscopic comparison between the 1° spectra at 1500 UT and 1745 UT leads to similar negative DSCDs, as expected from our scenario. The delay of the decrease of the 3°, 5° and 15° DSCDs (Figure 12) can be explained by the fact that the plume is initially still probed by these elevation viewing angles because the distance from Appledore Island to where the average light path crosses the plume is smaller. Later the plume also moves such that these light paths do not probe the plume anymore and their DSCDs also become negative.

[59] That inhomogeneous trace gas distributions can challenge the MAX-DOAS approach has also been described by *Heckel et al.* [2005] and *Leigh et al.* [2006] for urban areas. Our case, however, was found in an area removed from direct sources and we did not expect to see such an effect. The detailed analysis of the light path reveals that for trace gas layers above ~500 m altitude, a homogeneity on the scale of ~10 km has to be assumed. While in our case the effect was quite extreme, cases where the DSCDs do not become negative may be more difficult to identify. Our analysis also implies that the spatial scale at which inhomogeneities can be tolerated is smaller at lower altitudes, i.e., it is determined mostly by the geometry of the light paths closer to the instrument.

[60] It is interesting to investigate whether a vertical NO_2 profile similar to that of HCHO can be identified at 1500 UT on 11 July. The MAX-DOAS NO_2 DSCDs show a clear separation in elevation angle (Figure 15). Therefore there must be a sizable amount of NO_2 in the MBL to cause the DSCDs to strongly depend on the elevation viewing angle. To investigate the NO_2 profile we again tested various vertical concentration profiles (Figure 16), by comparing calculated and measured DSCDs.

[61] The initial profiles assumed NO_2 confined to the lowest 300 m of the MBL (profile 13 in Figure 16) and in a layer from 1 to 2 km altitude (profile 17, Figure 16). The opposite dependence of the DSCDs on elevation angle for these two profile (see insert in Figure 16) leads to the conclusion that a combination of the two profiles would describe the actual situation better. This is shown in profiles 19, 21, and 24 in Figure 16. The best agreement between

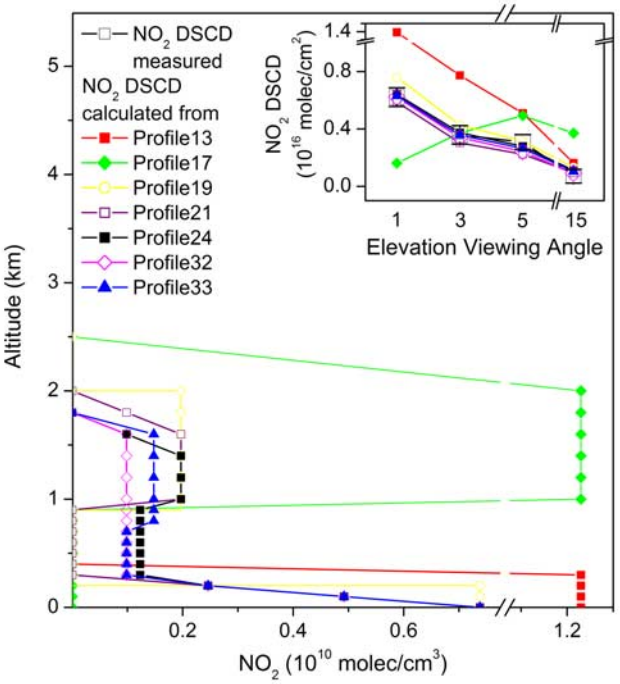

Figure 16. NO_2 vertical concentration profile used in the analysis of the MAX-DOAS observations on 11 July 2004, 1500 UT. Profile 24 fits the NO_2 observations best. Other vertical profiles used in the retrieval are also shown. The insert compares the NO_2 DSCDs calculated on the basis of the various profiles with the observations by the MAX-DOAS instrument.

measured and modeled DSCDs was found for profile 24 (Figure 16), which shows a linear decrease of the NO_2 concentration in the MBL, somewhat elevated NO_2 between 1 and 2 km, and no NO_2 above 2 km. To investigate how sensitive this result is to the variations of the concentration of the elevated layer we varied its concentration and width. Profiles 32 and 33 are examples of such variations. In general, the agreement is not very sensitive to changes in the range of ±50 ppt. On the basis of all tested profiles we can therefore put an uncertainty of ~50 ppt on the derived NO_2 concentrations at different altitudes.

[62] The shape of the derived profile is a result of the particular location and meteorology of the Isles of Shoals. The elevated surface NO_2 and its sharp decline with altitude in the lower MBL can be attributed to local NO_2 emissions, similar to those observed on 17 July. The mixing ratio observed by the MAX-DOAS in the lowest 100 m is ~300 ± 50 ppt, while the LP-DOAS observed 500 ± 160 ppt of NO_2. The MAX-DOAS surface mixing ratios immediately before and after 1500 UT were also retrieved on the basis of the aerosol profile "Trop9" (see Figure 15). The slightly higher LP-DOAS mixing ratios from 1430 to 1600 UT are most likely due to higher NO_2 levels in the lowest 50 m of the MBL due to local emissions. The elevated NO_2 aloft originates from continental outflow and can most likely be attributed to a small anthropogenic influence. The observed mixing ratios between 1 and 1.5 km altitude are ~100 ± 50 ppt. It is remarkable that the MAX-DOAS instrument can indeed identify and quantify such low levels of NO_2 above the MBL. We did not observe negative NO_2 DSCDs, as in the case of HCHO, because NO_2 was largely located in the MBL and was thus not influenced strongly by the movement of the layer above the MBL, as discussed above.

4. Conclusions

[63] Simultaneous multiaxis and long-path DOAS measurements were performed in summer 2004 at the Isles of Shoals in the Gulf of Maine. The retrieval of O_4, NO_2, and HCHO column densities from the MAX-DOAS measurements and the comparison of NO_2 and HCHO concentrations with LP-DOAS observations allowed the following conclusions about the capabilities and accuracy of the MAX-DOAS method.

[64] 1. Our results confirm previous studies [e.g., *Wagner et al.*, 2004] that MAX-DOAS O_4 observations can be used to gain information on the vertical distribution of the aerosol load, i.e., the aerosol extinction coefficient. This ability is crucial to constrain the radiative transfer calculations required for the trace gas retrieval. Our manual approach, which used one O_4 band together with meteorological information showed the potential of MAX-DOAS as an automatic ground-based remote sensing tool for aerosols. In a recent theoretical study, *Friess et al.* [2006] showed that expansion to more O_4 bands and the inclusion of the intensity will further improve this capability.

[65] 2. Ground-based MAX-DOAS is able to accurately measure trace gas concentrations at the surface under conditions where these gases are evenly distributed within the lower part of the mixed layer, i.e., in the absence of significant local sources. When trace gases are not evenly distributed in the mixed layer, MAX-DOAS retrieves vertically averaged concentrations and care has to be taken in the interpretation of these observations.

[66] 3. Vertical trace gas concentration profiles can be retrieved by MAX-DOAS, as shown in the example of a layer of elevated aerosol extinction and HCHO above the MBL. However, the interpretation of MAX-DOAS measurements is more challenging in this case and it is helpful to constrain the profiles with the meteorological or other observations.

[67] 4. Horizontal inhomogeneities in trace gas concentrations within the spatial range of the MAX-DOAS viewing geometry, i.e., ~13 km in our case for layers above the MBL, make the derivation of trace gas profiles difficult if not impossible without additional measurements. A possible solution for this problem would be the placement of another MAX-DOAS system at 5–10 km distance with a perpendicular line of sight, which would possibly provide enough information to constrain the retrieval.

[68] Our observations showed the applicability of MAX-DOAS as a remote sensing method for aerosols and trace gases. Considering the relative simplicity of the MAX-DOAS setup and the capability to operate fully automated and without assistance for extended periods of time, MAX-DOAS has the potential to become an important monitoring method in the future.

[69] **Acknowledgments.** We would like to thank the CHAiOS team and the staff at SML for their logistical support and Christoph von Friedeburg for valuable discussions on the radiative transfer calculations. Funding for this study was provided by the Atmospheric Chemistry Division of the National Science Foundation (ATM-0401599) and the Health of the Atmosphere Program of NOAA (RA133R-04-SE-0411). This paper is contribution 136 to the Shoals Marine Laboratory.

References

Alicke, B., U. Platt, and J. Stutz (2002), Impact of nitrous acid photolysis on the total hydroxyl radical budget during the Limitation of Oxidant Production/Pianura Padana Produzione di Ozono study in Milan, *J. Geophys. Res.*, *107*(D22), 8196, doi:10.1029/2000JD000075.

Aliwell, S. R., et al. (2002), Analysis for BrO in zenith-sky spectra: An intercomparison exercise for analysis improvement, *J. Geophys. Res.*, *107*(D14), 4199, doi:10.1029/2001JD000329.

Angevine, W. M., M. P. Buhr, J. S. Holloway, M. Trainer, D. D. Parrish, J. T. MacPherson, G. L. Kok, R. D. Schillawski, and D. H. Bowlby (1996a), Local meteorological featured affecting chemical measurements at a North Atlantic coastal site, *J. Geophys. Res.*, *101*(D22), 28,935–28,946.

Angevine, W. M., M. Trainer, S. A. McKeen, and C. M. Berkowitz (1996b), Mesoscale meteorology of the New England coast, Gulf of Maine, and Nova Scotia: Overview, *J. Geophys. Res.*, *101*(D22), 28,893–28,901.

Angevine, W. M., C. J. Senff, A. B. White, E. J. Williams, J. Koermer, S. T. K. Miller, R. Talbot, P. E. Johnston, S. A. McKeen, and T. Downs (2004), Coastal boundary layer influence on pollutant transport in New England, *J. Appl. Meteorol.*, *43*, 1425–1436.

Brauers, T., M. Hausmann, U. Brandenburger, and H.-P. Dorn (1995), Improvement of differential optical absorption spectroscopy with a multichannel scanning technique, *Appl. Opt.*, *34*(21), 4472–4479.

Friess, U., P. S. Monks, J. J. Remedios, A. Rozanov, R. Sinreich, T. Wagner, and U. Platt (2006), MAX-DOAS O_4 measurements: A new technique to derive information on atmospheric eorosols: 2. Modeling studies, *J. Geophys. Res.*, *111*, D14203, doi:10.1029/2005JD006618.

Greenblatt, G. D., J. J. Orlando, J. B. Burkholder, and A. R. Ravishankara (1990), Absorption measurements of oxygen between 330 and 1140 nm, *J. Geophys. Res.*, *95*(D11), 18,577–18,582.

Heckel, A., A. Richter, T. Tarsu, F. Wittrock, C. Hak, I. Pundt, W. Junkermann, and J. P. Burrows (2005), MAX-DOAS measurements of formaldehyde in the Po Valley, *Atmos. Chem. Phys.*, *5*, 909–918.

Hendrick, F., et al. (2006), Intercomparison exercise between different radiative transfer models used for the interpretation of ground-based zenith-sky and multi-axis DOAS observations, *Atmos. Chem. Phys.*, *6*, 93–108.

Henyey, L. C., and J. L. Greenstein (1941), Diffuse radiation in the galaxy, *Astrophys. J.*, *93*(1), 70–83.

Hönninger, G. (1999), Referenzspektren reaktiver Halogenverbindungen für DOAS-Messungen, Diploma Thesis, Univ. of Heidelberg, Heidelberg, Germany.

Hönninger, G. (2002), Halogen oxide study in the boundary layer by multi axis differential optical absorption spectroscopy and active longpath-DOAS, Ph.D. thesis, Univ. Heidelberg, Heidelberg, Germany.

Hönninger, G., and U. Platt (2002), Observations of BrO and its vertical distribution during surface ozone depletion at Alert, *Atmos. Environ.*, *36*, 2481–2489.

Hönninger, G., C. von Friedeburg, and U. Platt (2004a), Multi axis differential optical absorption spectroscopy (MAX-DOAS), *Atmos. Chem. Phys.*, *4*, 231–254.

Hönninger, G., H. Leser, O. Sebastian, and U. Platt (2004b), Ground-based measurements of halogen oxides at the Hudson Bay by active longpath DOAS and passive MAX-DOAS, *Geophys. Res. Lett.*, *31*, L04111, doi:10.1029/2003GL018982.

Leigh, R., G. Corlett, U. Friess, and P. S. Monks (2006), Concurrent multi-axis differential optical absorption spectroscopy system for the measurements of tropospheric nitrogen dioxide, *Appl. Opt.*, *45*(28), 7504–7518.

Meller, R., and G. K. Moorgat (2000), Temperature dependence of absorption cross sections of formaldehyde between 223 and 323 K in the wavelength range 225–375 nm, *J. Geophys. Res.*, *105*(D6), 7089–7101.

Miller, H. L., A. Weaver, R. W. Sanders, K. Arpag, and S. Solomon (1997), Measurements of arctic sunrise surface ozone depletion events at Kangerlussuaq, Greenland (67°N, 51°W), *Tellus, Ser. B*, *49*, 496–509.

Mount, G., R. Sanders, A. Schmeltekopf, and S. Solomon (1987), Visible spectroscopy at McMurdo station, Antarctica: 1. Overview and daily variation of NO_2 and O_3, Austral spring, *J. Geophys. Res.*, *92*, 8320–8328.

Noxon, J. F. (1975), Nitrogen dioxide in the stratosphere and troposphere measured by ground-based absorption spectroscopy, *Science*, *189*, 547–549.

Palmer, P. I., D. J. Jacob, A. M. Fiore, R. V. Martin, K. Chance, and T. P. Kurosu (2003), Mapping isoprene emissions over North America using formaldehyde column observations from space, *J. Geophys. Res.*, *108*(D6), 4180, doi:10.1029/2002JD002153.

Perliski, L. M., and S. Solomon (1993), On the evaluation of air mass factors for atmospheric near-ultraviolet and visible absorption spectroscopy, *J. Geophys. Res.*, *98*, 10,363–10,374.

Sanders, R. W., S. Solomon, M. A. Carroll, and A. L. Schmeltekopf (1988), Ground based measurements of O_3, NO_2, OClO and BrO during the Antarctic ozone depletion event, in *Ozone in the Atmosphere, Quadrennial Ozone Symposium 1988*, edited by R. D. Bjokov and P. Fabian, pp. 65–70, A. Deepak, Hampton, Va.

Shettle, E. P. (1989), Models of aerosols, clouds, and precipitation for atmospheric propagation studies, *AGARD Conf. Proc.*, *454*.

Sinreich, R., U. Frieβ, T. Wagner, and U. Platt (2005), Multi axis differential optical absorption spectroscopy (MAX-DOAS) of gas and aerosol distributions, *Faraday Disc.*, *130*, 153–164.

Solomon, S., A. L. Schmeltekopf, and R. W. Sanders (1987), On the interpretation of zenith sky absorption measurements, *J. Geophys. Res.*, *92*, 8311–8319.

Stutz, J., and U. Platt (1996), Numerical analysis and estimation of the statistical error of differential optical absorption spectroscopy measurements with least-squares methods, *Appl. Opt.*, *35*(30), 6041–6053.

Stutz, J., and U. Platt (1997), Improving long-path differential optical absorption spectroscopy with a quartz-fiber mode mixer, *Appl. Opt.*, *36*, 1105–1115.

Voigt, S., J. Orphal, K. Bogumil, and J. P. Burrows (2001), The temperature dependence (203–293 K) of the absorption cross sections of O_3 in the 230–850 nm region measured by Fourier-transform spectroscopy, *J. Photochem. Photobiol. A Chem.*, *143*, 1–9.

Voigt, S., J. Orphal, and J. P. Burrows (2002), The temperature and pressure dependence of the absorption cross-sections of NO_2 in the 250–800 nm region measured by Fourier-transform spectroscopy, *J. Photochem. Photobiol. A Chem.*, *149*, 1–7.

Volkamer, R., R. Spietz, J. Burrows, and U. Platt (2005), High-resolution absorption cross-section of glyoxal in the UV-visible and IR spectral range, *J. Photochem. Photobiol. A Chem.*, *172*, 35–46.

von Friedeburg, C. (2003), Derivation of trace gas information combining differential optical absorption spectroscopy with radiative transfer modeling, Ph.D. thesis, Univ. Heidelberg, Heidelberg, Germany.

von Friedeburg, C., T. Wagner, A. Geyer, N. Kaiser, B. Vogel, H. Vogel, and U. Platt (2002), Derivation of tropospheric NO_3 profiles using off-axis differential optical absorption spectroscopy measurements during sunrise and comparison with simulations, *J. Geophys. Res.*, *107*(D13), 4168, doi:10.1029/2001JD000481.

von Friedeburg, C., I. Pundt, K.-W. Mettendorf, T. Wagner, and U. Platt (2005), Multi-axis-DOAS measurements of NO_2 during the BAB II motorway emission campaign, *Atmos. Environ.*, *39*, 977–985.

Vountas, M., V. V. Rozanov, and J. P. Burrows (1998), Ring effect: Impact of rotational Raman scattering on radiative transfer in Earth's atmosphere, *J. Quant. Spectrosc. Radiat. Transfer*, *60*(6), 943–961.

Wagner, T., B. Dix, C. v. Friedeburg, U. Frieβ, S. Sanghavi, R. Sinreich, and U. Platt (2004), MAX-DOAS O_4 measurements: A new technique to derive information on atmospheric aerosols—Principles and information content, *J. Geophys. Res.*, *109*, D22205, doi:10.1029/2004JD004904.

Wahner, A., A. R. Ravishankara, S. P. Sander, and R. R. Friedl (1988), Absorption cross-section of BrO between 312 and 385 nm at 298 and 233 K, *Chem. Phys. Lett.*, *152*, 507–512.

Wittrock, F., H. Oetjen, A. Richter, S. Fietkau, T. Medeke, A. Rosanov, and J. P. Burrows (2003), MAX-DOAS measurements of atmospheric trace gases in Ny-Alesund, *Atmos. Chem. Phys. Disc.*, *3*, 6109–6145.

S. C. Hurlock, O. Pikelnaya, J. Stutz, and S. Trick, Department of Atmospheric and Oceanic Sciences, 7127 Math Sciences, University of California, Los Angeles, CA 90095-1565, USA. (jochen@atmos.ucla.edu)